PHYSICAL REVIEW B **109**, 224105 (2024)

Synergistic effects of pressure and hole doping on polymorphism of Ga_2O_3

Qiu-Shi Huang,[1] Xuefen Cai,[2,*] Xie Zhang,[3] Andrej Kuznetsov,[4] and Su-Huai Wei[1,†]
[1]*Beijing Computational Science Research Center, Beijing 100193, China*
[2]*State Key Laboratory of Radio Frequency Heterogeneous Integration (Shenzhen University), College of Physics and Optoelectronic Engineering, Shenzhen University, Shenzhen 518060, China*
[3]*School of Materials Science and Engineering, Northwestern Polytechnical University, Xi'an 710072, China*
[4]*Department of Physics, Centre for Materials Science and Nanotechnology, University of Oslo, P.O. Box 1048 Blindern, N-0316 Oslo, Norway*

(Received 14 July 2023; revised 25 April 2024; accepted 22 May 2024; published 7 June 2024)

Control of polymorphism in Ga_2O_3 poses a significant challenge. In this study, we investigate the phase stability and transitions of α-, β-, and κ-Ga_2O_3 structures using first-principles calculations. Our analysis of the pressure and energy relationship of Ga_2O_3 polymorphs demonstrates that external pressure can induce the transition from the ground-state monoclinic β to the corundum α phase, but not to the orthorhombic κ phases because of the small volumetric changes and relatively large energy differences. However, taking κ-Ga_2O_3 as an example, we propose that introducing holes (e.g., substituting Ga with a valence II ion) can stabilize the metastable phases in combination with pressure because the valence bands of the κ phase are higher than those in the α and β phases. These findings not only rationalize the absence of direct observation of the $\beta \rightarrow \kappa$ transitions with conventional external pressure, but also offer insights into the underlying physical mechanism behind the experimentally observed ion irradiation-induced transitions to metastable phases in Ga_2O_3.

DOI: 10.1103/PhysRevB.109.224105

I. INTRODUCTION

Gallium oxide (Ga_2O_3) with a wide band gap (4.2–5.3 eV) boasts a range of exceptional properties, including high breakdown field strength, high switching frequency, high temperature tolerance, and strong radiation resistance. These attributes make it an attractive candidate for a wide range of applications, including high-power electronic devices, day-blind ultraviolet communication systems, ultrasensitive gas detectors, and transparent ultraviolet electronic devices [1–5]. Ga_2O_3 has five recognized polymorphs, namely, α, β, γ, δ, and κ. Among these, the monoclinic β phase with space group $C2/m$ is the most stable form and, therefore, has been extensively studied [6–10]. The metastable phases have also attracted growing interest in recent years due to their appealing properties, e.g., orthorhombic κ-Ga_2O_3 has spontaneous polarization and ferroelectric behavior [11–17]. However, the process of stabilizing the metastable phases from β phase has not been a trivial work. External pressure has conventionally been used as an effective means for inducing phase changes in materials. For instance, it is experimentally reported that β-Ga_2O_3 can transform into corundum α-Ga_2O_3 by applying high pressure (4.4–19.2 GPa) [18–20]. Nevertheless, to date, direct observations of the transformation from the β to κ phases by applying pressure have not been reported. Surprisingly, it has been shown that ion implantation can trigger $\beta \rightarrow \kappa$ [21–23] transitions, although the underlying physical mechanism behind this phenomenon has not been clearly stated.

In this work, we perform a systematic first-principles investigation into the phase stability and transitions of α-, β-, κ-, and γ-Ga_2O_3 structures, which are commonly considered to have relatively low energies and high stabilities. We first explore the relationship between the energy and volume (pressure) of the Ga_2O_3 polymorphs and observe that the application of pressure does not induce the $\beta \rightarrow \kappa$ or $\beta \rightarrow \gamma$ phase transitions because the presence of the α phase with significantly small volume (large volume reduction) induces the $\beta \rightarrow \alpha$ phase transition *before* other phase transition occurs. Further, by investigating the $\beta \rightarrow \kappa$ phase transition as an example, we show that introducing holes (e.g., through ion implantation) can significantly lower the total energy of the κ-Ga_2O_3 phase due to its high valence band energy, thus stabilizing the κ-Ga_2O_3 with or without pressure, depending on the hole concentration. The findings presented here rationalize the experimentally observed $\beta \rightarrow \alpha$ phase transition induced by external pressure as well as other polymorph transitions caused by synergistic effect with ion irradiation.

II. COMPUTATIONAL METHOD

Our first-principles calculations are based on the projector augmented wave method and density functional theory with the Heyd-Scuseria-Ernzerhof hybrid functional [24] as implemented in the VASP code [25]. The Hartree-Fock exchange mixing parameter α is set to be 32% to match the experimentally observed band gaps. The Ga $3d$ electrons are treated as the valence electrons. We use a plane-wave basis set with a cutoff energy of 500 eV, and a Hellmann-Feynman force convergence criterion of 0.01 eV/Å for each atom. We sampled the Brillouin zone of α-, β-, γ-, and

---

[*] caixuefen@szu.edu.cn

[†] Present address: Eastern Institute of Technology, Ningbo 315200, China; suhuaiwei@eitech.edu.cn

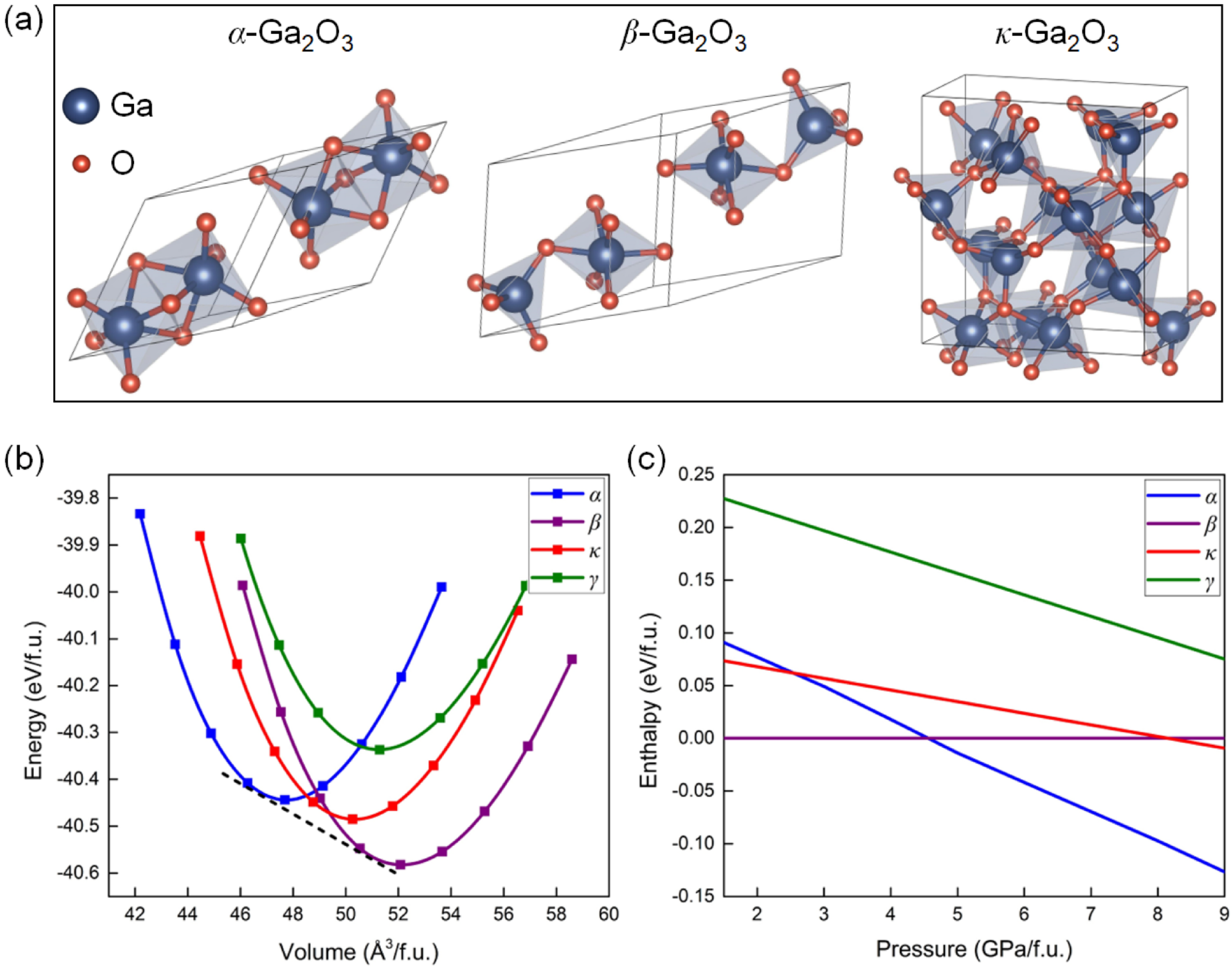

FIG. 1. (a) Primitive cells of α-, β-, and κ-Ga_2O_3. The γ phase with large unit cell and statistically occupied Ga sites is not plotted here. (b) Calculated energy-volume curves (E-V) for α-, β-, γ-, and κ-Ga_2O_3. The solid lines are fitted by the third-order Birch-Murnaghan equation of state. The dashed common-tangent line represents the allowed β-α phase transition by applying pressure. (c) Pressure dependence of the enthalpies for α-, γ-, and κ-Ga_2O_3 relative to β-Ga_2O_3 showing that the β-α phase transition occurs before other phase transitions can occur and the γ phase has much higher enthalpy compared to the other phases.

κ-Ga_2O_3 lattices with Γ-centered Monkhorst–Pack k grids with energy converged to 1 meV per formula unit, respectively. The band alignments between α-, β-, and κ-Ga_2O_3 are calculated using the three-steps approach described in Ref. [26]. In doping calculations, we constructed a supercell with 160 atoms for each phase and the hole doping is simulated by introducing holes without replacing Ga atoms with other atoms. Structural optimization is performed for all concentrations.

III. RESULTS AND DISCUSSION

Figure 1(b) presents the energy-volume (E-V) curves calculated for the α-, β-, γ-, and κ-Ga_2O_3 polymorphs. Given the structural disorder nature of γ-Ga_2O_3, in our calculation, we adopt the experimentally determined crystalline model detailed in Ref. [27]. The total energies are fitted to the third-order Birch-Murnaghan equation of state [28]. The ground-state properties extracted from Fig. 1(b), including lattice parameter, volume, and total energy per formula unit, for α-, β-, γ-, and κ-Ga_2O_3 are tabulated in Table I. Figure 1(a) depicts the corresponding atomic structures for the primitive cell of α-, β-, and κ-Ga_2O_3. α-Ga_2O_3 adopts the corundum structure with a space group of $R\bar{3}c$, where each Ga atom binds with six surrounding O atoms, forming a distorted GaO_6 octahedron. β-Ga_2O_3 has two nonequivalent Ga sites in a 1:1 ratio, with one site exhibiting tetrahedral and the other octahedral coordination geometry. γ-Ga_2O_3 exhibits a so-called defective spinel structure (cubic, $Fd\bar{3}m$) with both tetrahedral and octahedral coordination. It can be best described as a disordered phase derived from the β phase. κ-Ga_2O_3 crystallizes in the orthorhombic structure with a space group of $Pna2_1$, consisting of three nonequivalent Ga sites with octahedral, trigonal bipyramid, and tetrahedral coordination geometries in a 1:2:1 ratio, respectively.

The equilibrium volume increases from α- to κ- to γ- to β-Ga_2O_3. As expected, the monoclinic β structure has the lowest energy and is stable under ambient pressure for Ga_2O_3, consistent with prior calculations [11,23]. A common-tangent line can be constructed between the β and α phases, indicating a phase transition between these two phases can occur at the pressure given by the slope of the common-tangent

TABLE I. Calculated equilibrium lattice parameters (a, b, c), volume (V), total energy (E) per formula unit, and band gap (E_g) for α-, β-, γ-, and κ-Ga_2O_3. Experimental values for the band gap and lattice parameters of all three phases are provided in brackets. The space group for each phase is also given.

	α-Ga_2O_3	β-Ga_2O_3	γ-Ga_2O_3	κ-Ga_2O_3
Space group	$R\bar{3}c$	$C2/m$	$Fd\bar{3}m$	$Pna2_1$
a (Å)	5.00 (4.98[a])	12.22 (12.21[b])	8.228 (8.238[c])	5.02 (5.05[d])
b (Å)	5.00 (4.98[a])	3.03 (3.04[b])		8.65 (8.70[d])
c (Å)	13.47 (13.43[a])	5.79 (5.81[b])		9.26 (9.28[d])
V (Å/f.u.)	47.69	52.09	51.30	50.26
E (eV/f.u.)	−40.444	−40.582	−40.337	−40.485
E_g (eV)	5.29 (5.30[e])	4.84 (4.90[f])	4.05 (3.99[g])	4.94 (5.0[h])

[a] Reference [29].
[b] Reference [6].
[c] Reference [27].
[d] Reference [13].
[e] Reference [30].
[f] Reference [1].
[g] Reference [31].
[h] Reference [32].

line. To show it more clearly, the pressure dependence of the enthalpies for α-, γ-, and κ-Ga_2O_3 relative to β-Ga_2O_3 polymorph is illustrated in Fig. 1(c). The enthalpy of the α phase drops below that of the β phase after approximately 4.8 GPa, indicating that the β phase transforms into the α phase under such pressure conditions, in good agreement with previous experiments [18]. On the other hand, the enthalpies of the γ and κ phases are not the lowest ones at any pressure, suggesting that the phase transition to the γ and κ phases does not occur as pressure increases. This is attributed to the large volume of the γ- and κ-Ga_2O_3 as compared to that of α-Ga_2O_3. Because the γ phase has both high energy and large volume among the metastable phases, and as a disordered phase, the γ phase can be deduced from the β phase by varying temperature [27,33–35], rather than relying on pressure and doping, in the rest of the paper, we will only consider α-, β-, and κ-Ga_2O_3 phase transitions between the polymorphs.

The calculated projected electronic band structures of α-, β-, and κ-Ga_2O_3 in their respective ground states are shown in Fig. 2. The orthorhombic κ-Ga_2O_3 structure has four times as many bands per k point compared to that of the α and β phases due to its larger primitive unit cell containing 40 atoms. The conduction band minimums of all three phases are located at the Γ point, while the valence band maximum (VBM) states are located on the Γ-X line, L-I line (in agreement with Ref. [7]), and the Γ point for α-, β-, and κ-Ga_2O_3, respectively. The calculated band gaps, given in Table I, agree with the available experimental band gaps. Within the energy region between −5.0 and 0 eV, the O p character dominates the valence bands of all three phases. Meanwhile, in the region around −15 eV, the valence bands are primarily composed of Ga d states. It is noteworthy that the proportions of octahedral coordination geometry are 100%, 50%, and 25% for α-, β-, and κ-Ga_2O_3, respectively. As $p-d$ mixing at octahedral sites is symmetry forbidden or weak, it is expected that the $p-d$ coupling effect will increase from α to β to κ. Furthermore, the volume of the κ phase is about 96% of the β phase, and the VBM has high deformation potential due to the $p-d$ coupling, therefore, the reduction in volume in the κ phase will result in a stronger atomic $p-d$ repulsion than the β phase. These factors suggest that the VBM energy levels should increase from α to β to κ.

To verify this expectation, we calculate the band alignment between α-, β-, and κ-Ga_2O_3 using first-principles methods, as shown in Fig. 3(a). As anticipated, we see that the VBM energy increases in the sequence of α-, β-, and κ-Ga_2O_3. Furthermore, when holes are introduced into Ga_2O_3 phases, polarons are formed with the hole self-trapping energy (E_{st}) also increasing in the sequence of α-, β-, and κ-Ga_2O_3 [17]. Therefore, κ-Ga_2O_3, which has the highest VBM and E_{st} energy, can gain more energy with respect to the other two phases [36,37]. Therefore, it is plausible to stabilize the metastable κ phase by incorporating holes into Ga_2O_3. We substantiate this idea by computing the total energy for α-, β-, and κ-Ga_2O_3 as a function of the injected hole density, as depicted in Fig. 3(b). Here, the slopes correspond to the energy increase rate with the hole injection. We find that under low hole density, β-Ga_2O_3 has a

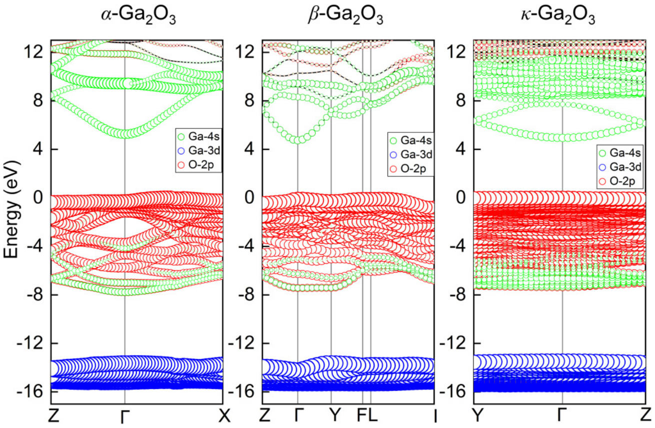

FIG. 2. Projected band structures of α-, β-, and κ-Ga_2O_3. The valence band maximum is set to zero.

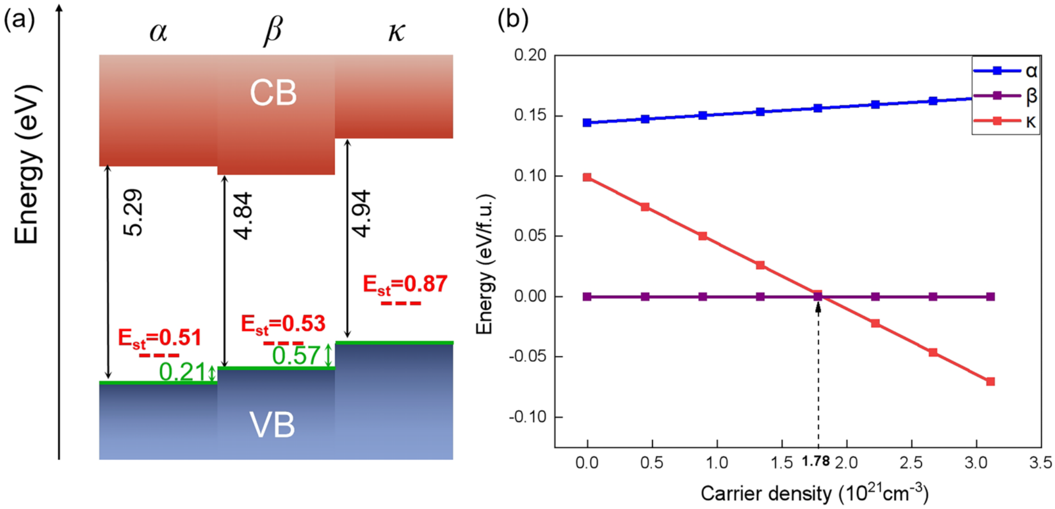

FIG. 3. (a) Calculated band alignments between α-, β-, and κ-Ga$_2$O$_3$. The green numbers represent the differences in the VBM between the various phases. The red dashed lines indicate the hole self-trapping energy (E_{st}) relative to the VBM of the Ga$_2$O$_3$ phases [17]. (b) Total energies of α- and κ-Ga$_2$O$_3$ as a function of the hole density relative to β-Ga$_2$O$_3$.

lower energy compared to κ-Ga$_2$O$_3$. However, the energies of the two phases approach each other with increasing hole incorporation. Notably, as the hole density reaches 1.78×10^{21} cm^{-3}, the energy of the κ phase becomes lower than that of the β phase, resulting in the stabilization of the κ phase. This finding offers an alternative explanation for the ion-implantation-induced metastable phase transitions observed experimentally [23]. It is also noticeable that the energy difference between the α and β phases increases with hole carrier density, which indicates that the required pressure to cause the β-α phase transition will increase with the introduced hole carrier density [13–15].

It is possible to use the synergistic effects of introducing holes and applying pressure to induce the phase transitions between the β-Ga$_2$O$_3$ to κ-Ga$_2$O$_3$ phases to reduce either the required hole concentration or the pressure. This is because when we introduce holes into these materials, due to the band alignment, the energy of α-Ga$_2$O$_3$ increases relative to that of β-Ga$_2$O$_3$, while the energy of κ-Ga$_2$O$_3$ decreases. Our calculations show that at the critical doping concentration of 3.56×10^{20} cm^{-3} and under a critical pressure of 5.7 GPa, a direct pressure-induced transition from β-Ga$_2$O$_3$ to κ-Ga$_2$O$_3$ to α-Ga$_2$O$_3$ phases becomes possible, as shown in Fig. 4. When the hole doping concentration increases beyond the critical concentration, the required pressure causing the β-phase to the κ-phase transition is reduced but the pressure for the further κ-phase to the α-phase transition will increase from the critical pressure of 5.7 GPa. It should be noted,

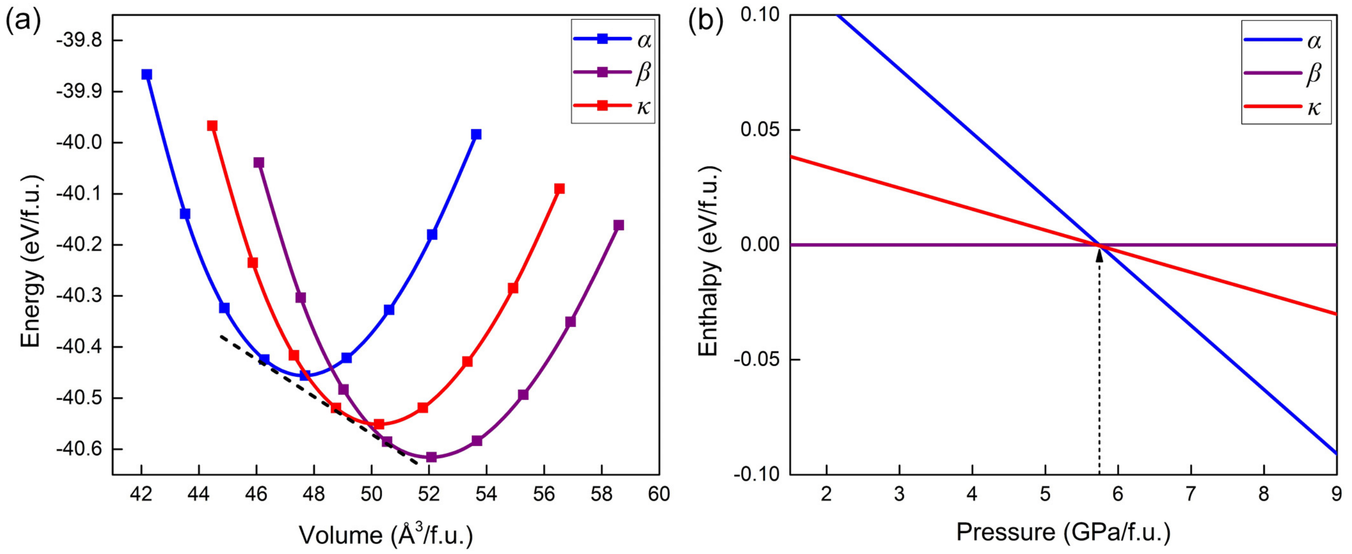

FIG. 4. (a) Calculated energy-volume curves (E-V) for α-, β-, and κ-Ga$_2$O$_3$ at a hole doping concentration of 3.56×10^{20} cm^{-3} where the three phases have the same enthalpy. The slope of the dashed common-tangent line (5.7 GPa) represents the β-κ-α phase transition. (b) Pressure dependence of the enthalpies for α- and κ-Ga$_2$O$_3$ relative to β-Ga$_2$O$_3$ at the same hole doping concentration.

even though the calculations of the electronic effects were performed for the $\beta \rightarrow \kappa$ phase transition, it is likely the $\beta \rightarrow \gamma$ transition may employ a similar mechanism.

IV. CONCLUSION

In conclusion, we have carried out a first-principles investigation on the phase stability and transitions of α-, β-, and κ-Ga_2O_3 structures. Our results reveal that pressure can induce the transformation of β phase to α phase, but it does not lead to either $\beta \rightarrow \kappa$ phase transitions. To shed light on the mechanism underlying the metastable polymorph transitions induced by ion implantation, we have analyzed the crystal structures, electronic structures, and band alignment of the κ-Ga_2O_3 in comparison with the α and β phases. We find that the κ-Ga_2O_3 phase exhibits a higher VBM and E_{st} state compared to the α and β phases, which can be attributed to its small volume and consequently strong $p-d$ coupling effect. Based on this observation, we demonstrate that introducing holes into the Ga_2O_3 systems, especially with the synergistic effect of pressure, can stabilize the metastable κ-Ga_2O_3 phases. Our findings provide a rational explanation for the experimental observations of the $\beta \rightarrow \alpha$ phase transition under external pressure and the metastable polymorph transitions under ion irradiation. Our study, thus provides insights on the synergistic effects of pressure and carrier doping in controlling the phase stability of crystals.

ACKNOWLEDGMENTS

This work was supported by the National Natural Science Foundation of China (Grants No. 12088101, No. 11991060, No. U2230402, and No. 12204471). The international collaboration was enabled in part via the INTPART Program at the Research Council of Norway through Project No. 322382. We acknowledge computational resources from the Beijing Computational Science Research Center.

[1] M. Orita, H. Ohta, M. Hirano, and H. Hosono, Appl. Phys. Lett. **77**, 4166 (2000).

[2] M. Baldini, Z. Galazka, and G. Wagner, Mater. Sci. Semicond. Process. **78**, 132 (2018).

[3] S. J. Pearton, J. Yang, P. H. Cary Iv, F. Ren, J. Kim, M. J. Tadjer, and M. A. Mastro, Appl. Phys. Rev. **5**, 011301 (2018).

[4] J. Y. Tsao *et al.*, Adv. Electron. Mater. **4**, 1600501 (2018).

[5] X. Cai, F. P. Sabino, A. Janotti, and S.-H. Wei, Phys. Rev. B **103**, 115205 (2021).

[6] J. Åhman, G. Svensson, and J. Albertsson, Acta Crystallogr., Sect. C: Struct. Chem. **52**, 1336 (1996).

[7] H. Peelaers and C. G. Van de Walle, Phys. Status Solidi B **252**, 828 (2015).

[8] J. L. Lyons, Semicond. Sci. Technol. **33**, 05LT02 (2018).

[9] H. Peelaers, J. L. Lyons, J. B. Varley, and C. G. Van de Walle, APL Mater. **7**, 022519 (2019).

[10] M. J. Tadjer, J. L. Lyons, N. Nepal, J. A. Freitas, A. D. Koehler, and G. M. Foster, ECS J. Solid State Sci. Technol. **8**, Q3187 (2019).

[11] S. Yoshioka, H. Hayashi, A. Kuwabara, F. Oba, K. Matsunaga, and I. Tanaka, J. Phys.: Condens. Matter. **19**, 346211 (2007).

[12] M. B. Maccioni and V. Fiorentini, Appl. Phys. Express **9**, 041102 (2016).

[13] I. Cora, F. Mezzadri, F. Boschi, M. Bosi, M. Čaplovičová, G. Calestani, I. Dódony, B. Pécz, and R. Fornari, CrystEngComm **19**, 1509 (2017).

[14] J. Kim, D. Tahara, Y. Miura, and B. G. Kim, Appl. Phys. Express **11**, 061101 (2018).

[15] R. Batra, H. D. Tran, B. Johnson, B. Zoellner, P. A. Maggard, J. L. Jones, G. A. Rossetti, Jr., and R. Ramprasad, Chem. Mater. **32**, 3823 (2020).

[16] J. Lee, H. Kim, L. Gautam, and M. Razeghi, Crystals **11**, 446 (2021).

[17] J. L. Lyons, ECS J. Solid State Sci. Technol. **8**, Q3226 (2019).

[18] J. P. Remeika and M. Marezio, Appl. Phys. Lett. **8**, 87 (1966).

[19] K. E. Lipinska-Kalita, B. Chen, M. B. Kruger, Y. Ohki, J. Murowchick, and E. P. Gogol, Phys. Rev. B **68**, 035209 (2003).

[20] M. Yan-Mei, C. Hai-Yong, Y. Kai-Feng, L. Min, C. Qi-Liang, L. Jing, and Z. Guang-Tian, Chin. Phys. Lett. **25**, 1603 (2008).

[21] A. Azarov, V. Venkatachalapathy, E. V. Monakhov, and A. Y. Kuznetsov, Appl. Phys. Lett. **118**, 232101 (2021).

[22] D. Tetelbaum *et al.*, Mater. Lett. **302**, 130346 (2021).

[23] A. Azarov, C. Bazioti, V. Venkatachalapathy, P. Vajeeston, E. Monakhov, and A. Kuznetsov, Phys. Rev. Lett. **128**, 015704 (2022).

[24] J. Heyd, G. E. Scuseria, and M. Ernzerhof, J. Chem. Phys. **118**, 8207 (2003).

[25] G. Kresse and J. Furthmüller, Phys. Rev. B **54**, 11169 (1996).

[26] L. Lang, Y.-Y. Zhang, P. Xu, S. Chen, H. J. Xiang, and X. G. Gong, Phys. Rev. B **92**, 075102 (2015).

[27] H. Y. Playford, A. C. Hannon, M. G. Tucker, D. M. Dawson, S. E. Ashbrook, R. J. Kastiban, J. Sloan, and R. I. Walton, J. Phys. Chem. C **118**, 16188 (2014).

[28] T. Katsura and Y. Tange, Minerals **9**, 745 (2019).

[29] M. Marezio and J. P. Remeika, J. Chem. Phys. **46**, 1862 (1967).

[30] D. Shinohara and S. Fujita, Jpn. J. Appl. Phys. **47**, 7311 (2008).

[31] T. Chen and K. Tang, Appl. Phys. Lett. **90**, 053104 (2007).

[32] S. Krishna, Y. Lu, C.-H. Liao, V. Khandelwal, and X. Li, Appl. Surf. Sci. **599**, 153901 (2022).

[33] C. O. Areán, A. L. Bellan, M. P. Mentruit, M. R. Delgado, and T. G. Palomino, Microporous Mesoporous Mater. **40**, 35 (2000).

[34] S.-W. Kim, S. Iwamoto, and M. Inoue, Ceram. Interfaces **35**, 1603 (2009).

[35] H. Y. Playford, A. C. Hannon, E. R. Barney, and R. I. Walton, Chem. Eur. J. **19**, 2803 (2013).

[36] X. Cai, H.-X. Deng, and S.-H. Wei, Phys. Rev. B **103**, 245202 (2021).

[37] G. M. Dalpian, Y. Yan, and S.-H. Wei, Appl. Phys. Lett. **89**, 011907 (2006).